International Research Journal of Pharmacy and Medical Sciences
ISSN (Online): 2581-3277

Development of a FA-PLGA-PEG Loaded 3-Br-Benzyl-Noscapine Nanoparticle for Targeted Delivery into Breast Cancer Cell Lines: Chemical Synthesis and Experimental Validation

Namita Bhoi[1], Srinivas Kantevari[2], Pradeep Kumar Naik[1]*
[1]Centre of Excellence in Natural Product and Therapeutics, Department of Biotechnology and Bioinformatics, Sambalpur University, Odisha-768019, India
[2]Fluoro-Agrochemicals Division, CSIR-Indian Institute of Chemical Technology, Hyderabad, 500007, India
Email address: pknaik1973@suniv.ac.in

***Abstract*—*Folate-conjugated PLGA-PEG (FPP) nanocarrier is a promising strategy for targeted delivery of drug to enhanced anticancer efficacy by selective targeting of folate receptors, which are commonly overexpressed in breast cancer cells. We have assessed the anticancer efficacy of one of our previously created noscapine derivatives, N-3-Br-benzyl-noscapine, which we have incorporated into an FPP nanocarrier using the co-precipitation technique. DLS analysis of the nanocarrier revealed a hydrodynamic diameter of 155 ± 2 nm and a PDI of 0.27, indicating a uniform nanosize and suitability for tumor targeting via folate receptor-mediated uptake. Further, SEM images revealed aggregated spherical particles with a uniform distribution, suggesting good formulation stability. The cytotoxic potential of the FPP loaded with 3-Br-Bn-Nos was assessed in MDA-MB-231, T47D, and MCF-7 breast cancer cell lines and demonstrated a concentration-dependent reduction in cell viability. Against MDA-MB-231, MCF-7 and T47D cell lines, the IC_{50} values of FPP loaded 3-Br-Bn-Nos were found to be 37.2, 28.9 and 22.7 µg/mL, respectively which were significantly outperforming free 3-Br-Bn-Nos (IC_{50} values were 73.6, 59.8 and 54.1µg/mL, respectively). Cellular studies further revealed improved uptake of 3-Br-Bn-Nos by nanocarrier and disruption of the mitochondrial membrane potential, increased reactive oxygen species (ROS) generation and induction of apoptosis to cancer cells. In addition, a spheroid disintegration assay using a 3D tumor model mimicking the tumor microenvironment revealed partial shrinkage by day 5, with a noticeable but moderate reduction in overall size and density. This observation supports the enhanced therapeutic potential of FPP loaded 3-Br-Bn-Nos in effectively disrupting the tumor spheroid architecture compared with the free drug. Furthermore, in vivo toxicity assessment was conducted in rats to evaluate the safety of the formulation. Both acute and subacute toxicity studies confirmed that the FPP loaded 3-Br-Bn-Nos was well tolerated at the administered dose and exhibited no significant systemic toxicity. Collectively, these findings underscore the therapeutic potential of FPP loaded 3-Br-Bn-Nos in breast cancer therapy.*

***Keywords*—** *Breast cancer; FA-PLGA-PEG nanocarrier; Folate receptor; N-3-Br-benzyl-noscapine; 3D spheroid.*

I. Introduction

Advancements in nanomedicine have transformed the landscape of modern pharmacotherapy by offering innovative solutions for drug delivery challenges, particularly in oncology. Among the diverse nanocarrier systems, polymeric nanoparticles (PNs) have garnered significant attention because of their ability to encapsulate hydrophobic drugs, enhance their solubility, provide controlled release, and offer site-specific targeting. [1], [2] These nanosystems, especially those designed with tunable size and surface characteristics, exploit the enhanced permeability and retention (EPR) effect, allowing for passive accumulation in tumor tissues. [3], [4] Moreover, surface functionalization with targeting ligands further refines their selectivity, enabling active targeting of tumor-specific biomarkers while minimizing systemic toxicity. [5]

A well-established example of such a nanocarrier system is poly(lactic-co-glycolic acid) (PLGA), which is functionalized with polyethylene glycol (PEG) and folic acid (FA). This tri-block configuration (FA-PLGA-PEG) offers several advantages: PEG improves the pharmacokinetic profile by evading immune clearance, whereas FA facilitates active targeting via folate receptor-mediated endocytosis, which is particularly relevant in breast and ovarian cancers, where folate receptors are commonly overexpressed. [6], [7], [8] In contrast, these receptors are largely absent in normal tissues, reducing off-target uptake and associated toxicity.

In this study we have selected one of our previously developed halogenated derivatives of the natural alkaloid noscapine i.e. N-3-Br-benzyl-noscapine (3-Br-Bn-Nos) (Fig. 1) for targeted delivery to cancer cell lines. It has been established as a potent microtubule-targeting agent that induced mitotic arrest and apoptosis, making it a promising candidate for cancer therapy. [9] However, its poor aqueous solubility and potential systemic toxicity limit its clinical translation [10], [11]. While previous approaches, such as cyclodextrin complexation and lipid-based formulations, have been employed to address these limitations in colon and lung cancers, respectively, a folate-targeted polymeric system (FA-PLGA-PEG) has not yet been explored. [12], [13]

To address this gap, the present study focuses on the encapsulation of 3-Br-Bn-Nos using FA-PLGA-PEG (FPP) nanocarrier and experimental evaluation based on cellular study. The FPP nanocarrier was developed via an emulsion–solvent evaporation technique and optimized for

Namita Bhoi, Srinivas Kantevari, and Pradeep Kumar Naik, "Development of a FA-PLGA-PEG Loaded 3-Br-Benzyl-Noscapine Nanoparticle for Targeted Delivery into Breast Cancer Cell Lines: Chemical Synthesis and Experimental Validation," *International Research Journal of Pharmacy and Medical Sciences (IRJPMS)*, Volume 8, Issue 5, pp. 18-26, 2025.

high drug loading, sustained release, and colloidal stability. The incorporation of folic acid as a surface ligand aims to enhance selective uptake by cancer cells while reducing systemic side effects. This work not only introduces a novel formulation strategy for 3-Br-Bn-Nos but also demonstrates the utility of receptor-mediated nanocarrier systems in enhancing the therapeutic index of poorly soluble anticancer agents.

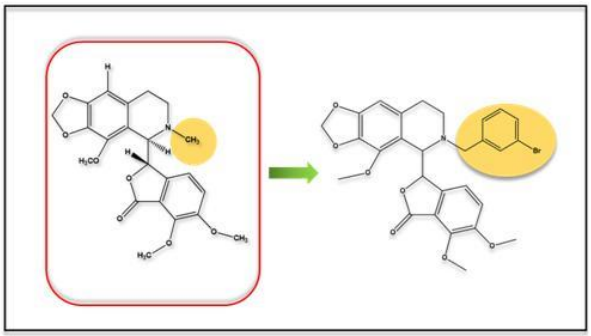

Fig. 1. Schematic representation of the structural modification of noscapine to obtain 3-bromobenzyl-substituted N-imidazopyridine noscapinoid (3-Br-Bn-Nos).

II. Materials and Methods

A. Materials and Reagents

Poly(lactic-co-glycolic acid) (PLGA), polyethylene glycol-bis(amine) (PEG-bis-amine), and folic acid (FA) were used for the synthesis of PLGA-PEG-FA nanocarrier. Coupling agents such as N,N′-dicyclohexylcarbodiimide (DCC) and N-hydroxysuccinimide (NHS) were employed for the conjugation reactions. Solvents, including anhydrous dimethyl sulfoxide (DMSO), anhydrous dichloromethane (DCM) and methanol, were used during nanoparticle formulation. The 3-(4,5-dimethylthiazol-2-yl)-2,5-diphenyltetrazolium bromide (MTT) test was used to determine the cells' viability. All chemicals and reagents were purchased from Sigma-Aldrich (USA) unless stated differently. Throughout the study, deionized and filtered water (Milli-Q Academic®, Millipore, Molsheim, France) was used in all the experimental procedures.

B. Cell Culture

Breast cancer cell lines MCF-7, MDA-MB-231, and T47D (obtained from NCCS, Pune) were grown at 37°C in a humidified incubator with 5% CO2. The cell culture utilized Dulbecco's Modified Eagle Medium (DMEM) (Gibco BRL, UK) supplemented with fetal bovine serum (FBS) (Gibco BRL, UK), along with 10X phosphate-buffered saline (PBS) (Gibco BRL, UK), 0.25% trypsin containing 0.003% EDTA (Gibco BRL, UK), and a penicillin/streptomycin solution (10 mg/mL, Sigma–Aldrich). Dimethyl sulfoxide (DMSO) (HIMEDIA) was used for treatment preparation. All the experimental procedures were conducted under sterile conditions inside a Class A2 biosafety cabinet, adhering strictly to aseptic conditions.

C. Chemical Synthesis of 3-Br-benzyl Noscapine (3-Br-Bn-Nos):

A derivative of Noscapine, 3-Br-benzyl Noscapine was chemically synthesised as reported earlier. [9] Briefly the starting solution of Noscapine (200 mg, 0.50 mmol) in acetone (5 mL), was added to potassium carbonate (1.10 mmol), potassium iodide (0.5 mmol) and 3-Bromo-benzyl bromide (0.55 mmol) and stirred at room temperature (RT) for 1 h. The crude reaction mixture was filtered and evaporated under vacuum, water (5 mL) and dichloromethane (2 X 10 mL) were added, and the organic layer was dried over Na_2SO_4 and concentrated under reduced pressure. The crude residue was purified via silica gel column chromatography with hexane/ethyl acetate (70:30) to yield a solid product of 3-Br-Bn-Nos. It was completely characterised using NMR, HRMS and IR spectroscopy. The detailed synthetic scheme is mentioned below.

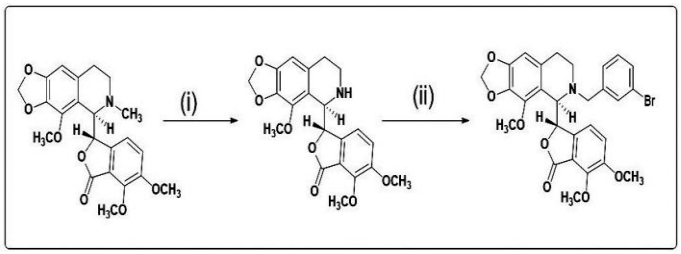

Reaction Scheme: Reaction Conditions: (i) a: m-CPBA, DCM; b: 2 N HCl; C: $FeSO_4.7H_2O$; (ii) 3-Bromo benzyl bromide, KI, K_2CO_3, acetone, RT, 96% yield.

(S)-3-((R)-6-(3-bromobenzyl)-4-methoxy-5,6,7,8tetrahydro-[1,3]dioxolo[4,5-g]isoquinolin-5-yl)-6,7dimethoxyisobenzofuran-1(3H)-one:Yield: 97%; mp 65°C; [α]D25 = 52.0 (c = 1, Dichloromethane); IR νmax (cm^{-1}): 3503, 2940, 2837, 1759, 1621, 1498, 1387, 1271, 1212, 1039, 891, 785, 695. ^{1}HNMR: (300 MHz, $CDCl_3$): δ 7.40-7.30 (m, 2H), 7.24-7.09 (m, 2H), 6.99 (d, J= 8.30 Hz, 1H), 6.34 (s, 1H), 6.15 (d, J= 8.30 Hz, 1H), 5.95 (s, 2H), 5.66 (d, J= 3.96 Hz, 1H), 4.60 (d, J= 3.96 Hz, 1H), 4.17-4.06 (m, 4H), 4.04 (s, 3H) 3.87, (s, 3H), 3.63 (d, J= 13.78 Hz, 1H), 2.50-2.37 (m, 2H), 2.32-2.19 (m, 1H), 2.07-1.92 (m, 1H). ^{13}CNMR (75 MHz, $CDCl_3$): δ 168.1, 152.2, 148.5, 147.9, 141.5, 140.4, 134.0, 131.8, 131.4, 130.0, 129.7, 127.3, 122.2, 118.1, 117.7, 116.6, 102.4, 100.7, 81.6, 81.1, 62.5, 61.1, 59.5, 59.3, 56.7, 45.4, 26.8. MS (ESI) m/z 568 $[M+H]^+$. HRMS (ESI) Calcd for $C_{28}H_{26}BrNO_7$ $[M+H]^+$: 568.41, found: 568.41.

D. Synthesis of the FA-PLGA-PEG Nanocarrier

The FA-PLGA-PEG nanocarrier (FPP) was synthesized following a previously established method with minor modifications, as illustrated in Fig. 2. [14], [15]

1) PLGA Activation

PLGA was dissolved in dry dichloromethane (DCM), and N-hydroxysuccinimide (NHS) and N,N′-dicyclohexylcarbodiimide (DCC) were added at a 1:2:2 molar ratio (PLGA:NHS:DCC). The reaction was carried out under an inert argon atmosphere at room temperature for 24 hours with continuous stirring. After the reaction was finished, the mixture was filtered to get rid of the by-product, dicyclohexylurea (DCU). The filtrate was added drop wise to

Namita Bhoi, Srinivas Kantevari, and Pradeep Kumar Naik, "Development of a FA-PLGA-PEG Loaded 3-Br-Benzyl-Noscapine Nanoparticle for Targeted Delivery into Breast Cancer Cell Lines: Chemical Synthesis and Experimental Validation," *International Research Journal of Pharmacy and Medical Sciences (IRJPMS)*, Volume 8, Issue 5, pp. 18-26, 2025.

ice-cold diethyl ether to precipitate the product. To get rid of any unreacted NHS, the resulting solid was rinsed repeatedly with a cold combination of ether and methanol. The activated PLGA was collected and vacuum-dried.

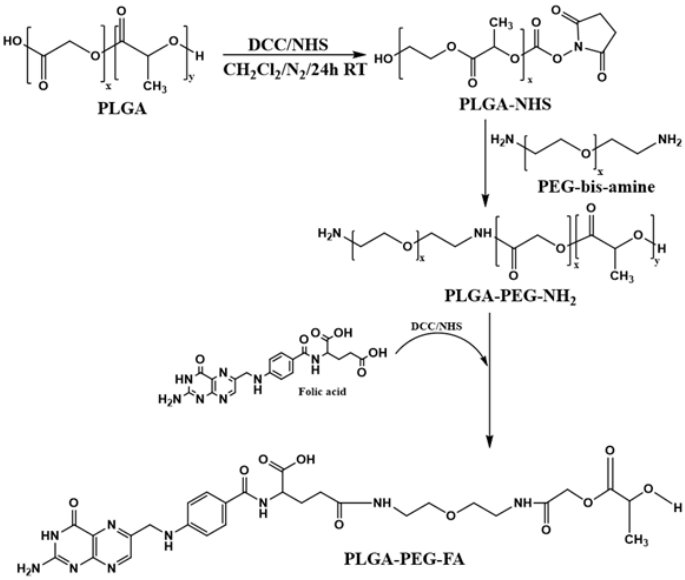

Fig. 2. Synthetic scheme for the preparation of the FA-PLGA-PEG nanocarrier.

2) PEG Conjugation to Activated PLGA

The NHS-activated PLGA was redissolved in dry DCM and added drop wise to a separately prepared solution of PEG-bis(amine) in DCM. A 1:3 molar ratio (PLGA:PEG) was used to minimize the formation of undesired triblock structures. With mild mixing, the process went on for 24 hours at room temperature in an argon environment. The resulting mixture was precipitated in chilled methanol. The copolymer PLGA-PEG-NH_2 was purified by repeated methanol washes, followed by vacuum drying.

3) Folic Acid Activation

Folic acid was reacted with NHS and DCC at a 1:2:2 molar ratio in anhydrous DMSO, with a catalytic amount of triethylamine. The reaction was carried out overnight under an argon atmosphere in the absence of light. After filtration to remove DCU, the activated folic acid was precipitated in ice-cold anhydrous ether, washed, and vacuum-dried to obtain the NHS-activated folic acid derivative.

4) Coupling of Folic Acid to PLGA-PEG

NHS-activated folic acid was dissolved in dry DMSO and added drop wise to a stirred solution of PLGA-PEG-NH_2 in DMSO, maintaining a 1:1 molar ratio (FA: PLGA-PEG-NH_2). The reaction was allowed to proceed for 24 hours at room temperature under an inert atmosphere under light-protected conditions. After completion, the product was precipitated in ice-cold diethyl ether, filtered, and washed repeatedly to remove unreacted components. The resulting FPP nanocarrier was vacuum-dried and stored under desiccation until further use.

E. Loading of 3-Br-Bn-Nos onto FPP Nanocarrier

3-Br-Bn-Nos was loaded onto FPP nanocarrier via the nanoprecipitation method. Briefly, 50 mg of the FPP nanocarrier and 5 mg of 3-Br-Bn-Nos (maintaining a 10% drug-to-polymer ratio) were co-dissolved in 5 mL of acetone. This organic phase was slowly introduced into 25 mL of an aqueous solution of 1% (w/v) polyvinyl alcohol (PVA), followed by probe sonication at 37% amplitude for 1 minute, with 10-second ON/OFF pulse cycles. To aid in the complete evaporation of the acetone, the emulsion was then mixed for six hours at 500 RPM. After evaporation, the dispersion was sonicated once more time and centrifuged at 20,000 rpm for 45 minutes at 4 °C. The resulting nanoparticle pellet was washed three times with deionized water and subsequently lyophilized. The FPP-loaded 3-Br-Bn-Nos nanoparticle was prepared in triplicate for consistency.

F. Structural and Chemical Characterization of FPP-loaded 3-Br-Bn-Nos Nanoparticle

1) Particle Size Determination via Dynamic Light Scattering (DLS)

To determine the particle size of the nanoparticle, the FPP-loaded 3-Br-Bn-Nos was diluted in deionized water and subjected to ultrasonication in a bath sonicator. The measurements were carried out at 25 °C using a Litesizer DLS 500 instrument. Each sample was evaluated through 30 measurement runs, each performed in triplicate. The average hydrodynamic diameter and polydispersity index (PDI) were calculated.

2) Morphological Analysis by Scanning Electron Microscopy (SEM)

The surface characteristics, morphology, and size distribution of the FPP-loaded 3-Br-Bn-Nos nanoparticle was analyzed using field-emission scanning electron microscopy (FE-SEM; JEOL JSM-6480 LV). The samples were adhered to aluminium stubs using conductive carbon tape, followed by gold sputter coating under an argon atmosphere (SC 7620, Quorum Technologies, UK). Imaging was conducted at an accelerating voltage of 10 kV with a working distance of 4.1 mm under high vacuum conditions.

3) Drug Encapsulation Efficiency

The drug loading capacity of the FPP nanocarrier was assessed by quantifying the amount of 3-Br-Bn-Nos remaining in the supernatant after centrifugation of the nanoparticle dispersion. This unbound drug amount was subtracted from the total amount of drug initially used. All measurements were conducted in triplicate using a validated UV–Vis spectrophotometric method at a wavelength of 309 nm. The encapsulation efficiency was calculated using the following formula:

$$EE\ (\%) = ((\text{Total Drug} - \text{Free Drug})/\text{Total Drug}) \times 100$$

4) In Vitro Drug Release Study

Drug release profiles of FPP nanocarrier was investigated in phosphate-buffered saline (PBS, pH ~7.4). The FPP-loaded 3-Br-Bn-Nos (5 mg each) nanoparticle was suspended in 20 mL of PBS and stirred continuously at 150 rpm at 37 °C. At selected intervals (ranging from 5 minutes to 48 hours), 2 mL of the medium was collected and replaced with fresh PBS to

Namita Bhoi, Srinivas Kantevari, and Pradeep Kumar Naik, "Development of a FA-PLGA-PEG Loaded 3-Br-Benzyl-Noscapine Nanoparticle for Targeted Delivery into Breast Cancer Cell Lines: Chemical Synthesis and Experimental Validation," *International Research Journal of Pharmacy and Medical Sciences (IRJPMS)*, Volume 8, Issue 5, pp. 18-26, 2025.

maintain sink conditions. The drug concentration was measured spectrophotometrically at 312 nm. [16], [17], [18]

G. In Vitro Cytotoxicity Assay

An MTT assay was employed to evaluate the cytotoxic effects of the free 3-Br-Bn-Nos and FPP-loaded 3-Br-Bn-Nos nanoparticle on the MDA-MB-231, MCF-7 and T47D breast cancer cell lines. The cells were plated in 96-well plates at 5×10^3 cells/well and allowed to attach for 24 hours. The cells were then treated with the test samples at different concentrations (5, 10, 50, 75, and 100 µg/mL) for 48–72 hours. MTT reagent (0.5 mg/mL) was added, and the mixture was incubated for 4 hours. Then, the formazan crystals were dissolved in DMSO, and the absorbance was measured at 570 nm. Untreated cells served as negative controls. [19]

H. Nuclear Morphology Assessment by Hoechst 33342

MDA-MB-231 cells was treated with IC_{50} concentrations of 3-Br-Bn-Nos and FPP-loaded 3-Br-Bn-Nos for 24 hours. The cells were washed with PBS, fixed in 100% ice-cold methanol for 15 minutes, and then stained with Hoechst 33342 (1 µg/mL) for 15 minutes. Fluorescent nuclear changes were examined under a Nikon ECLIPSE Ts2R microscope. [20]

I. Mitochondrial Membrane Potential (MMP) Evaluation Using JC-1

JC-1 dye was used to assess changes in the mitochondrial membrane potential (MMP). The cells were treated with IC_{50} concentration of 3-Br-Bn-Nos and FPP-loaded 3-Br-Bn-Nos for 24 hours. Following treatment, the cells were washed, stained with 5 µM JC-1 for 30 minutes at 37°C, and imaged. Red (J-aggregates) and green (monomers) fluorescence was quantified to assess mitochondrial depolarization using a Nikon ECLIPSE Ts2R microscope.

J. ROS Generation Assay Using DCF-DA

Reactive oxygen species (ROS) within the cells were quantified using DCF-DA. A 10 mM DCF-DA stock in DMSO was diluted to a working concentration of 20 µM. MDA-MB-231 cells treated with IC_{50} concentrations of 3-Br-Bn-Nos and FPP-loaded 3-Br-Bn-Nos for 12 hours were incubated with 20 µM DCF-DA for 30 minutes at 37°C. Fluorescence was visualized via microscopy and quantified with a Hitachi F-7000 spectrofluorometer after lysis. [21]

K. 3D Spheroid Disintegration Assay

To replicate tumor microenvironments in vivo, MDA-MB-231 cells (1x103 cells/well) were cultured in 96-well round-bottom dishes with extremely low adherence. The plates were subsequently centrifuged at 1000 rpm for 10 minutes and incubated for 7–10 days to form compact spheroids. The spheroids were then treated with 3-Br-Bn-Nos and FPP-loaded 3-Br-Bn-Nos. The medium was replaced every 48 hours. The spheroids were observed over 5 days for disintegration and size reduction using a Nikon inverted phase-contrast microscope. Spheroid size was quantified using ImageJ.

L. Acute Toxicity Evaluation in Rats

To determine the acute oral toxicity of 3-Br-Bn-Nos and FPP-loaded 3-Br-Bn-Nos, a single dose of varying concentrations (250, 500, 1000, 2000, or 5000 mg/kg body weight) was administered to Wistar rats. The animals were given one of the specified dosages orally after being split into six groups (n = 6 animals in each group). For 14 days, the rats were kept under constant surveillance for indications of toxicity or death. The total number of deaths in each group was recorded at the end of the observation period, in accordance with OECD Guideline No. 425 (2022).

M. Subacute Toxicity Assessment of 3-Br-Bn-Nos and FPP-loaded 3-Br-Bn-Nos Nanoparticle

For subacute toxicity evaluation, Wistar rats were randomly assigned to three groups of six animals each (n = 6). The Group-1 was the control and treated with 1% saline water. Group-2 and Group-3 were the treated groups and were administrated with 3-Br-Bn-Nos and FPP-loaded 3-Br-Bn-Nos nanoparticle orally at a dose of 500 mg/kg body weight per day for 28 consecutive days following OECD guidelines. During this period, the animals were observed daily for any signs of illness, behavioural abnormalities, or mortality. Parameters such as body weight, food consumption, and water intake were recorded throughout the study.

N. Haematological and Biochemical Analysis

At the end of the subacute study, the animals were anaesthetized via mild isoflurane followed by cervical dislocation. Blood samples were collected via cardiac puncture. A complete blood count (CBC) was performed via an automated hematology analyser (Byovet). For biochemical analysis, the serum was separated by centrifuging the blood at 5000 rpm for 10 minutes via an Eppendorf 5810r centrifuge. Various biochemical markers, including glucose (GLU), albumin (ALB), urea, creatinine (CREA), cholesterol (CHOL), triglycerides (TG), SGPT, SGOT, total protein (TP), HDL, and alkaline phosphatase (ALP), were measured using an automated biochemical analyser (Byovet Smart-5DX) with standard diagnostic kits.

O. Histopathological Examination via H&E Staining

Histological evaluation was conducted on major organs such as the brain, heart, liver, and kidneys collected from rats to identify any potential toxic effects. The tissues were fixed in 10% neutral buffered formalin, dehydrated through a graded alcohol series, cleared with xylene, and embedded in paraffin. Following established procedures, hematoxylin and eosin (H&E) staining was applied to 3.5 µm thick sections of the paraffin blocks. To look for histopathological changes in the stained areas, a Nikon ECLIPSE Ts2R inverted microscope was used for microscopic examination.

III. Results and Discussion

A. Physicochemical Characterization of FPP-loaded 3-Br-Bn-Nos Nanoparticle

1) Particle Size and Morphology

DLS analysis revealed a hydrodynamic diameter of 155 ± 2 nm and a PDI of 0.27 for the FPP-loaded 3-Br-Bn-Nos

Namita Bhoi, Srinivas Kantevari, and Pradeep Kumar Naik, "Development of a FA-PLGA-PEG Loaded 3-Br-Benzyl-Noscapine Nanoparticle for Targeted Delivery into Breast Cancer Cell Lines: Chemical Synthesis and Experimental Validation," *International Research Journal of Pharmacy and Medical Sciences (IRJPMS)*, Volume 8, Issue 5, pp. 18-26, 2025.

nanoparticle, indicating a uniform nanosize and suitability for tumor targeting via both the EPR effect and folate receptor-mediated uptake. SEM images (Fig. 3a) revealed aggregated spherical particles with a uniform distribution, suggesting good formulation stability.

2) Entrapment Efficiency

UV–visible spectroscopic analysis revealed a high drug entrapment efficiency of 98.7% of FPP nanocarrier. This finding suggests a strong interaction between 3-Br-Bn-Nos and FPP, which may enhance delivery efficiency and therapeutic potential.

3) In Vitro Drug Release

Drug release in PBS (pH 7.4) revealed that free 3-Br-Bn-Nos was rapidly released (~100% within 2 h), whereas FPP-loaded 3-Br-Bn-Nos nanoparticle exhibited a sustained release pattern with ~65% drug release over 72 h (Fig. 3b).

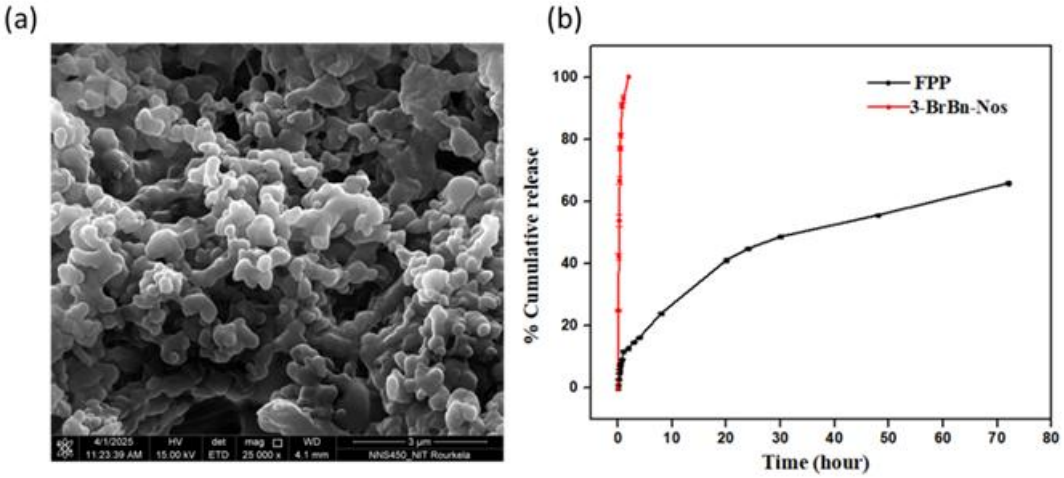

Fig. 3. (a) Representative SEM image of FPP-loaded 3-Br-Bn-Nos nanoparticles. (b) *In vitro* release profile of 3-Br-Bn-Nos from FPP nanocarrier vs. free 3-Br-Bn-Nos release in PBS (pH 7.4).

B. FPP Nanocarrier Increased the Cytotoxicity of 3-Br-Bn-Nos

The cytotoxic potential of the FPP-loaded 3-Br-Bn-Nos was assessed in three different breast cancer cell lines such as MDA-MB-231, T47D, and MCF-7. The cytotoxicity effect was demonstrated in a concentration-dependent manner (Fig. 4). The IC_{50} value using MDA-MB-231 for FPP-loaded 3-Br-Bn-Nos was found to be 37.2 µg/mL which is significantly outperformed compared to free 3-Br-Bn-Nos with IC_{50} of 73.6 µg/mL (Fig. 4a). Similarly, against MCF-7 the IC_{50} value for FPP-loaded 3-Br-Bn-Nos was found to be 28.9 µg/mL compared to free 3-Br-Bn-Nos with IC_{50} of 59.8 µg/mL, (Fig. 4b). In the case of T47D, the IC_{50} value of FPP-loaded 3-Br-Bn-Nos was 22.7 µg/mL in comparison to the free 3-Br-Bn-Nos with IC_{50} value of 54.1 µg/mL (Fig. 4c). The improvement in IC_{50} value for FPP-loaded 3-Br-Bn-Nos is attributed primarily to folate receptor-mediated targeting and greater cellular uptake of the drug.

C. FPP-loaded 3-Br-Bn-Nos Triggered Cellular Alterations Leading to Apoptosis

Hoechst 33342 staining (Fig. 4d) revealed clear differences in nuclear morphology among the treatment groups. The cells exposed to the FPP-loaded 3-Br-Bn-Nos displayed prominent apoptotic features, such as intense chromatin condensation and marked nuclear fragmentation. In contrast, cells treated with free 3-Br-Bn-Nos presented only moderate nuclear alterations, whereas untreated control cells presented uniformly stained nuclei with a healthy, intact morphology. The pronounced apoptotic effects by the FPP-loaded 3-Br-Bn-Nos treated cells suggested that the nanoparticle system significantly enhances the intracellular delivery and antitumour activity of 3-Br-Bn-Nos compared to the free drug.

D. FPP-loaded 3-Br-Bn-Nos Induced Greater Mitochondrial Membrane Depolarization Than Free 3-Br-Bn-Nos

The effects of FPP-loaded 3-Br-Bn-Nos on the mitochondrial membrane potential (MMP) compared to free 3-Br-Bn-Nos was assessed using JC-1 staining (Fig. 5a). In untreated control cells, JC-1 primarily formed red fluorescent aggregates within healthy mitochondria, indicating preservation of the MMP and a low green/red fluorescence ratio. The green/red fluorescence ratio increased somewhat as a result of therapy with 3-Br-Bn-Nos, suggesting that the mitochondrial membrane was partially depolarized. In contrast, cells exposed to FPP-loaded 3-Br-Bn-Nos presented a significant increase in the green/red fluorescence ratio, reflecting a substantial decrease in the MMP. These findings suggest that FPP-loaded 3-Br-Bn-Nos causes a more pronounced disruption of mitochondrial function, thereby enhancing apoptosis more effectively than both the control and the free drug. Overall, these data support the superior proapoptotic activity of FPP-loaded 3-Br-Bn-Nos through mitochondrial destabilization.

E. FPP-loaded 3-Br-Bn-Nos Results in Greater ROS-Mediated Apoptotic Activity Compared to 3-Br-Bn-Nos

Reactive oxygen species (ROS) are crucial mediators of intracellular signalling and are key drivers of apoptosis. The production of intracellular ROS was evaluated in cells treated with FPP-loaded 3-Br-Bn-Nos and 3-Br-Bn-Nos. Cells treated

Namita Bhoi, Srinivas Kantevari, and Pradeep Kumar Naik, "Development of a FA-PLGA-PEG Loaded 3-Br-Benzyl-Noscapine Nanoparticle for Targeted Delivery into Breast Cancer Cell Lines: Chemical Synthesis and Experimental Validation," *International Research Journal of Pharmacy and Medical Sciences (IRJPMS)*, Volume 8, Issue 5, pp. 18-26, 2025.

with FPP-loaded 3-Br-Bn-Nos showed markedly higher green fluorescence compared to those treated with 3-Br-Bn-Nos, indicating increased ROS production (Fig. 5b). The increased ROS production was associated with increased mitochondrial damage, loss of membrane potential, and activation of apoptosis-related pathways, including caspase signalling. These findings underscore the pivotal role of ROS in driving apoptosis and highlight the enhanced proapoptotic efficacy of FPP-loaded 3-Br-Bn-Nos over the free drug.

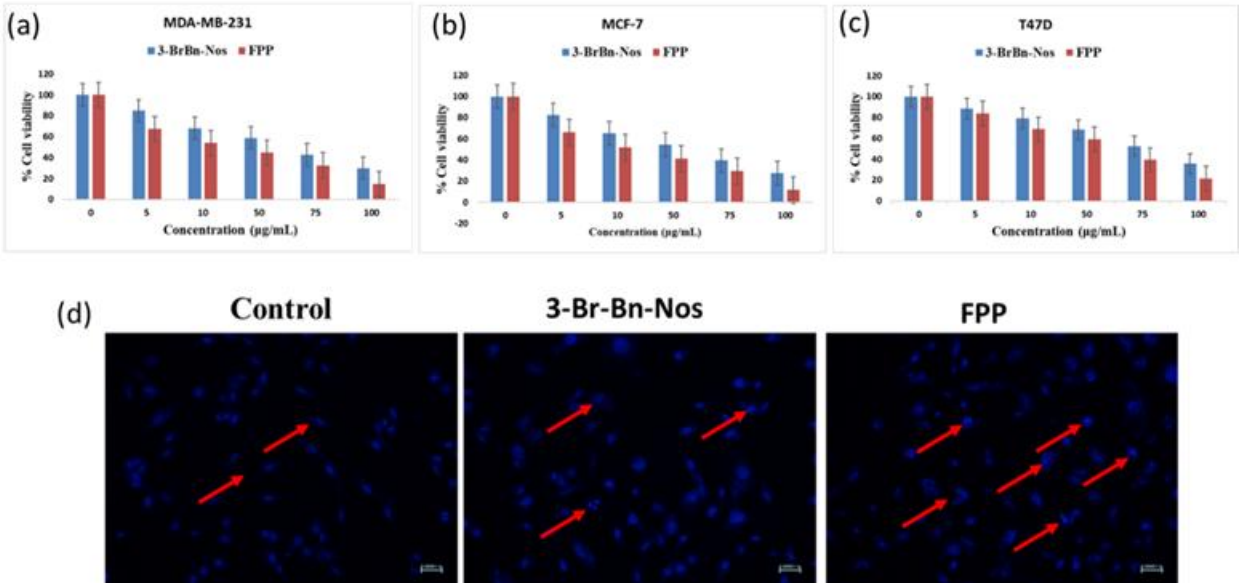

Fig. 4. Dose-dependent cytotoxic effects of 3-Br-Bn-Nos and FPP-loaded 3-Br-Bn-Nos on (a) MDA-MB-231, (b) MCF-7 and (c) T47D breast cancer cell lines. Cell viability was assessed using the MTT assay after 48 h of treatment at various concentrations (0–100 µM). The data are presented as the means ± SDs (n = 3). (d) Representative Hoechst 33342 staining images of MDA-MB-231 cells showing nuclear condensation and fragmentation in treated cells, indicating the induction of apoptosis following exposure to the free drug and FPP-loaded 3-Br-Bn-Nos.

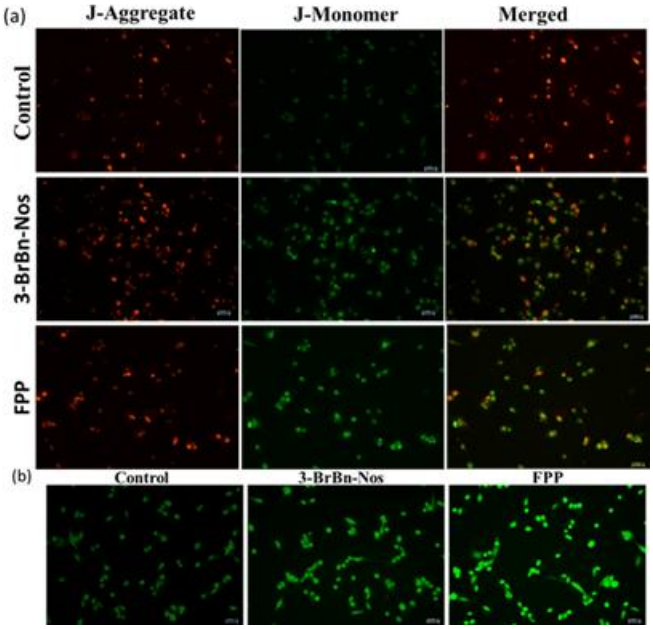

Fig. 5. Representative fluorescence images showing (a) the mitochondrial membrane potential (MMP) in MDA-MB-231 cells as assessed by JC-1 staining. A decrease in the red/green fluorescence ratio indicates MMP disruption after treatment with 3-Br-Bn-Nos and its nanoparticle formulation (FPP). (b) ROS generation in MDA-MB-231 cells visualized by DCFDA staining, where increased green fluorescence reflects elevated ROS levels (n=3).

F. Disruption of Tumor Spheroids Following Treatment With 3-Br-Bn-Nos and FPP-loaded 3-Br-Bn-Nos Nanoparticles

The ability of 3-Br-Bn-Nos and FPP-loaded 3-Br-Bn-Nos nanoparticles to disrupt 3D tumor spheroids was visually examined over a 5-day period. The images depicted a clear contrast in spheroid morphology across treatment groups. In the control group, the spheroids retained their dense and compact structure from day 1 to day 5, showing no signs of

Namita Bhoi, Srinivas Kantevari, and Pradeep Kumar Naik, "Development of a FA-PLGA-PEG Loaded 3-Br-Benzyl-Noscapine Nanoparticle for Targeted Delivery into Breast Cancer Cell Lines: Chemical Synthesis and Experimental Validation," *International Research Journal of Pharmacy and Medical Sciences (IRJPMS)*, Volume 8, Issue 5, pp. 18-26, 2025.

structural disintegration. Upon treatment with 3-Br-Bn-Nos, the spheroids exhibited partial shrinkage by day 5, with a noticeable but moderate reduction in overall size and density. In stark contrast, FPP-loaded 3-Br-Bn-Nos treated spheroids displayed substantial disintegration and loss of structural integrity by day 5, with a visibly smaller and more fragmented core than the other groups did (Fig. 6). These observations support the enhanced therapeutic potential of FPP nanoparticles in effectively disrupting the tumor spheroid architecture compared with the free drug after 5 days of administration.

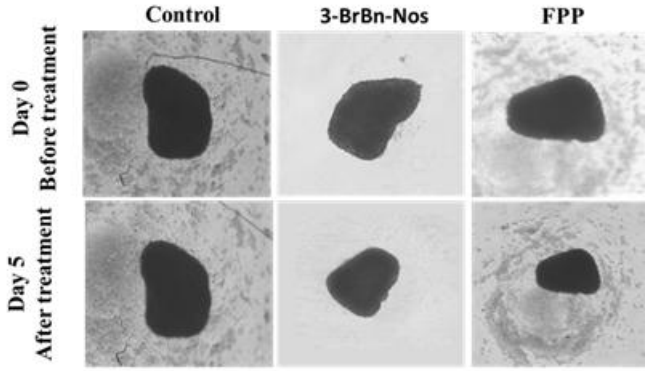

Fig. 6. Representative phase-contrast images show the structural integrity of the tumor spheroids following treatment with 3-Br-Bn-Nos and FPP-loaded 3-Br-Bn-Nos nanoparticles for 5 days. Untreated spheroids served as controls.

TABLE 1. Body weights (in grams) of rats treated with the control, 3-Br-Bn-Nos, and FPP-loaded 3-Br-Bn-Nos nanoparticle at a daily dose of 500 mg/kg body weight for 28 days.

Days	Body weight (grams)		
	Control	3-Br-Bn-Nos	FPP-loaded 3-Br-Bn-Nos
1	241.174±1.097	241.177±0.589	241.803±0.595
7	244.041±1.12	243.363±1.301	243.857±0.97
14	246.055±0.995	246.373±0.786	246.823±0.874
21	247.871±0.529	247.832±0.474	248.238±0.443
28	249.607±0.9	249.275±1.026	249.314±0.839

G. Acute and Subacute Toxicity of 3-Br-Bn-Nos and FPP-loaded 3-Br-Bn-Nos in Rats

The acute oral toxicity of 3-Br-Bn-Nos and its FPP nanoformulation was evaluated in Wistar rats according to OECD guidelines. A single dose of each test substance was administered, and the animals were observed over a 14-day period for any signs of mortality, behavioural changes, body weight variation, or organ-related toxicity. No mortality or significant behavioural abnormalities were detected in any of the treatment groups, including the control, during the observation period. For the subacute toxicity assessment, the rats received daily oral doses of 3-Br-Bn-Nos, FPP-loaded 3-Br-Bn-Nos or vehicle (control) for 28 consecutive days. The animals were closely monitored for clinical symptoms; changes in body weight; food and water intake; as well as haematological, biochemical, and histopathological parameters. No treatment-related mortality or observable toxicity symptoms were reported throughout the study duration. All treated groups, including the control, presented a progressive increase in body weight, suggesting preserved metabolic and physiological functions. Detailed measurements of body weight (Table 1), food and water consumption (Table 2) were documented to support these findings.

TABLE 2. Food (in grams) and water intake (in mL) of rats treated with the control, 3-Br-Bn-Nos, or its nanoparticle formulation (FPP) at a daily dose of 500 mg/kg body weight for 28 days.

Food intake			
Day	Control	3-Br-Bn-Nos	FPP-loaded 3-Br-Bn-Nos
1	21.461±0.442	22.311±0.821	20.958±0.961
7	23.509±0.913	23.434±0.911	23.715±0.943
14	24.696±0.448	24.903±0.368	25.087±0.333
21	26.203±0.665	26.901±0.621	25.9±0.71
28	28.817±1.028	28.313±0.815	29.575±0.322
Water intake			
1	20.809±0.352	20.869±0.656	20.88±0.578
7	22.104±0.689	21.718±0.482	21.49±0.319
14	23.132±0.596	22.9±0.651	22.592±0.333
21	24.08±0.427	24.219±0.481	24.613±0.336
28	24.762±0.477	25.473±0.344	25.27±0.221

H. Haematological and Biochemical Parameters Following Treatment with 3-Br-Bn-Nos and FPP-loaded 3-Br-Bn-Nos

A 28-day subacute toxicity study was conducted to assess the hematological and biochemical effects of 3-Br-Bn-Nos and FPP-loaded 3-Br-Bn-Nos nanoparticle in rats. Parameters such as RBC count, hemoglobin (Hb), hematocrit (HCT), MCV, WBC count, and platelet levels were evaluated. No significant changes were observed in RBC, Hb, HCT, or red cell indices (MCV, MCH, MCHC), indicating normal erythropoiesis and red blood cell morphology.

TABLE 3. The haematological parameters of the rats treated with 3-Br-Bn-Nos and FPP-loaded 3-Br-Bn-Nos at a daily dose of 500 mg/kg body weight for 28 days showed no significant differences compared to the untreated control group.

Parameter	Control	3-Br-Bn-Nos	FPP-loaded 3-Br-Bn-Nos
White blood cell count (WBC) (10^3/L)	6.575±0.863	6.756±0.285	6.478±0.38
Neutrophils (Neu#) (10^3/L)	5.642±0.889	6.061±0.792	5.629±0.498
Lymphocytes (Lym#) (10^3/L)	2.262±0.918	2.46±0.477	2.512±0.767
Monocytes (Mon#) (10^3/L)	1.604±0.332	1.351±0.201	1.257±0.308
Eosinophils (Eos#) (10^3/L)	0.594±0.304	0.306±0.272	0.477±0.267
Basophil (Bas#) (10^3/L)	0.429±0.34	0.508±0.146	0.589±0.245
NLR	2.515±0.987	2.72±0.691	2.456±0.851
PLR	1.244±0.529	1.163±0.102	1.443±0.258
red blood cell count (RBC) (10^{12}/L)	5.864±0.578	5.782±0.503	5.921±0.487
Hemoglobin (HGB) (g/dL)	15.823±1.755	14.741±1.45	14.694±1.150
HCT	44.067±3.428	43.43±4.412	45.453±3.559
MCV (fL)	82.048±3.042	80.949±2.69	81.452±3.440
MCH (pg)	31.689±1.645	31.729±1.479	31.780±2.864
MCHC (g/L)	33.724±0.469	33.23±0.852	34.135±1.133
RDW-CV	12.907±0.799	12.438±1.412	13.340±1.551
RDW-SD (fL)	44.111±2.543	40.976±4.145	42.817±2.521
platelet count (PLT) (10^3/L)	155.659±2.545	153.616±2.735	155.514±1.366
PCT (mL/L)	1.407±0.293	1.542±0.363	1.705±0.343

Namita Bhoi, Srinivas Kantevari, and Pradeep Kumar Naik, "Development of a FA-PLGA-PEG Loaded 3-Br-Benzyl-Noscapine Nanoparticle for Targeted Delivery into Breast Cancer Cell Lines: Chemical Synthesis and Experimental Validation," *International Research Journal of Pharmacy and Medical Sciences (IRJPMS)*, Volume 8, Issue 5, pp. 18-26, 2025.

The WBC and differential leukocyte counts remained within physiological limits, suggesting that there was no immune suppression or inflammatory response. The platelet counts also revealed no adverse effects on coagulation. Biochemical analyses revealed no significant differences in serum glucose, total protein, albumin, globulin, or electrolytes (Na^+, K^+, Ca^{2+}, P) between the treated and control groups. Liver enzymes (ALP, ALT, AST) remained within normal ranges, indicating no hepatotoxicity. Similarly, renal function markers (urea and creatinine) were not abnormal. The results are presented in Table 3 and Table 4.

TABLE 4. The serum biochemical parameters of the rats treated with 3-Br-Bn-Nos and FPP-loaded 3-Br-Bn-Nos at a daily dose of 500 mg/kg body weight for 28 days showed no significant alterations compared to the untreated control group.

Parameter	Control	3-Br-Bn-Nos	FPP-loaded 3-Br-Bn-Nos
Glucose (GLU)	77.792±1.556	77.042±2.021	77.240±1.523
Albumin (ALB)	4.175±0.626	3.875±0.681	3.578±0.644
Urea (UREA)	18.555±2.4	18.484±2.294	18.768±2.243
Creatinine (CREA)	1.365±0.231	1.385±0.261	1.580±0.312
Cholestrol (CHOL)	165.36±11.02	140.907±27.472	142.79±23.46
Triglycerides (TG)	49.85±4.43	47.206±4.538	48.006±4.238
Alanine Transaminase (ALT)	16.86±4.731	15.801±4.548	15.568±3.723
Aspartate Aminotransferase (AST)	6.995±2.632	5.59±2.771	5.550±2.672
Total Protein (TP)	7.277±0.653	7.186±0.693	7.434±0.524
Magnesium (MG)	2.453±0.245	2.481±0.31	2.834±0.573
Phosphorus (PHOS)	4.542±0.807	5.002±1.036	5.487±1.12
Calcium (CA)	10.769±0.371	10.551±0.795	10.09±0.65
Direct Bilirubin (DBIL)	0.572±0.255	0.518±0.27	0.545±0.773
Total Bilirubin (TBIL)	0.595±0.195	0.685±0.134	0.597±0.211
High-density Lipoprotein (HDL)	38.724±1.568	38.69±1.168	38.672±1.303
Gamma-glutamyl Transferase (GGT)	4.454±3.011	4.763±2.427	4.543±2.781
Alkaline Phosphatase (ALP)	107.343±2.615	106.776±1.968	105.96±1.864

I. Histopathological Evaluation of Vital Organs via Hematoxylin & Eosin (HE) Staining

Histopathological assessment of vital organs, including the brain, heart, kidneys, lungs, and liver, was carried out after 28 days of daily oral treatment with 3-Br-Bn-Nos and FPP-loaded 3-Br-Bn-Nos at 500 mg/kg. Tissue sections from treated rats were compared with those from control animals to evaluate any structural alterations (Fig. 7). The brain tissue exhibited intact neuronal architecture without signs of neurotoxicity. Cardiac sections revealed well-preserved myocardial fibres, indicating that there were no cardiotoxic effects. Kidney histology revealed normal glomeruli and tubules, suggesting preserved renal function. Similarly, liver sections maintained their lobular structure, with no signs of inflammation, necrosis, or fatty changes. Overall, no significant histopathological abnormalities were observed in the treated groups, supporting the safety and biocompatibility of 3-Br-Bn-Nos and FPP-loaded 3-Br-Bn-Nos at the tested dose.

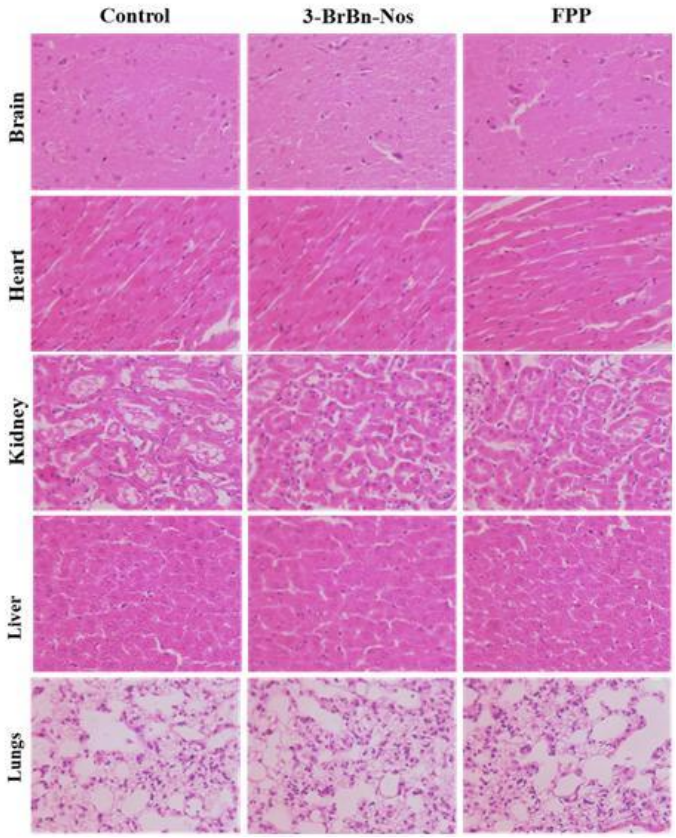

Fig. 7. Representative histological sections of major organs (heart, brain, kidney, liver, and lungs) were stained with hematoxylin and eosin (H&E) and observed at 40x magnification.

IV. Conclusion

The present study highlights the potential of 3-bromo-benzyl noscapine (3-Br-Bn-Nos) as an effective anticancer agent and demonstrates that its therapeutic performance is significantly improved through folate-targeted polymeric nanoparticle (FPP) delivery. Despite its inherent poor aqueous solubility, the nanoformulation enabled better solubility, enhanced cellular uptake, and a marked reduction in the IC_{50} across the tested cancer cell lines while sparing normal cells. Mechanistic studies revealed the induction of apoptosis, mitochondrial dysfunction, and ROS generation in cancer cells, which was supported by the results of morphological and functional assays. Additionally, 3D spheroid disintegration assays further confirmed its potency in a more physiologically relevant model. The *in vivo* evaluation confirmed that FPP did not induce any significant hematological, biochemical, or histopathological abnormalities, confirming its safety. Overall, this study establishes 3-Br-Bn-Nos-loaded FPP as a promising and biocompatible anticancer formulation with improved bioavailability and targeted therapeutic efficacy.

Acknowledgments

N.B. thanks DST-INSPIRE for the fellowship (IF190506). We acknowledge the Centre of Excellence in Natural Products and Therapeutics (COE-NPT) and DBT-BUILDER for funding. We acknowledge the Central Instrumentation Facility (CIF) at

Sambalpur University for providing the dynamic light scattering facility.

Conflict of Interest

The authors declare that they have no conflicts of interest.

Data Availability Statement

The data that support the findings of this study are available upon request from the corresponding author.

Ethical Approval: The animal experiment was approved by the Institutional Animals Ethics Committee (25/12/217-CPCSEA).

REFERENCES

[1] J. K. Patra, "Nano based drug delivery systems: Recent developments and future prospects," 2018.

[2] D. Peer, J. M. Karp, S. Hong, O. C. Farokhzad, R. Margalit, and R. Langer, "Nanocarriers as an emerging platform for cancer therapy," 2007.

[3] M. Chehelgerdi, "Progressing nanotechnology to improve targeted cancer treatment: overcoming hurdles in its clinical implementation," 2023.

[4] Z. He, Y. Zhang, and N. Feng, "Cell membrane-coated nanosized active targeted drug delivery systems homing to tumor cells: A review," 2020.

[5] R. Bajracharya, "Functional ligands for improving anticancer drug therapy: current status and applications to drug delivery systems," *Drug Deliv*, vol. 29, no. 1, 2022.

[6] J. Chen, "Dual tumor-targeted poly(lactic-co-glycolic acid)–polyethylene glycol–folic acid nanoparticles: A novel biodegradable nanocarrier for secure and efficient antitumor drug delivery," *Int J Nanomedicine*, vol. 12, 2017.

[7] H. K. Makadia and S. J. Siegel, "Poly Lactic-co-Glycolic Acid (PLGA) as biodegradable controlled drug delivery carrier," *Polymers (Basel)*, vol. 3, no. 3, 2011.

[8] H. S. Yoo and T. G. Park, "Folate-receptor-targeted delivery of doxorubicin nano-aggregates stabilized by doxorubicin-PEG-folate conjugate," *Journal of Controlled Release*, vol. 100, no. 2, 2004.

[9] S. G. Dash, S. Kantevari, S. K. Pandey, and P. K. Naik, "Synergistic interaction of N-3-Br-benzyl-noscapine and docetaxel abrogates oncogenic potential of breast cancer cells," *Chem Biol Drug Des*, vol. 98, no. 3, 2021.

[10] G. M. Calaf, L. A. Crispin, and E. O. Quisbert-Valenzuela, "Noscapine and Apoptosis in Breast and Other Cancers," 2024.

[11] S. Kumar, B. Sagar, A. Gaur, S. Shukla, E. Pandey, and S. Gulati, "Insight into the Tubulin-Targeted Anticancer Potential of Noscapine and its Structural Analogs," *Anticancer Agents Med Chem*, vol. 23, no. 6, 2022.

[12] J. Madan, "Inclusion complexes of noscapine in β-cyclodextrin offer better solubility and improved pharmacokinetics," *Cancer Chemother Pharmacol*, vol. 65, no. 3, 2010.

[13] S. Gandhi and I. Roy, "Lipid-Based Inhalable Micro- and Nanocarriers of Active Agents for Treating Non-Small-Cell Lung Cancer," 2023.

[14] M. M. El-Hammadi, Á. V. Delgado, C. Melguizo, J. C. Prados, and J. L. Arias, "Folic acid-decorated and PEGylated PLGA nanoparticles for improving the antitumour activity of 5-fluorouracil," *Int J Pharm*, vol. 516, no. 1–2, 2017.

[15] H. Fasehee, "Delivery of disulfiram into breast cancer cells using folate-receptor-targeted PLGA-PEG nanoparticles: In vitro and in vivo investigations," *J Nanobiotechnology*, vol. 14, no. 1, 2016.

[16] Z. Zhang and S. S. Feng, "The drug encapsulation efficiency, in vitro drug release, cellular uptake and cytotoxicity of paclitaxel-loaded poly(lactide)-tocopheryl polyethylene glycol succinate nanoparticles," *Biomaterials*, vol. 27, no. 21, 2006.

[17] S. M. Jusu, "Plga-cs-peg microparticles for controlled drug delivery in the treatment of triple negative breast cancer cells," *Applied Sciences (Switzerland)*, vol. 11, no. 15, 2021.

[18] Lewis DJ, On the interaction of copper(II) with disulfiram. *Chemical Communications (Camb)*, vol. 50, no. 87, 13334–7, 2014.

[19] N. Bhoi, D.R. Sahoo, E. Naik, A. Pradhan, M. Mishra, L.K. Pradhan, S. Rath, N.R. Nayak, P.K. Naik "Exploring the therapeutic potential of *Eulophia nuda* tuber by integrating phytochemical analysis with anticancer and antimicrobial efficacy, and in vivo safety profiling." *Journal of Herbs, Spices & Medicinal Plants*, 2025.

[20] M. Ponselvi Induja, D. Ezhilarasan, and N. Ashok Vardhan, "*Evolvulus alsinoides* methanolic extract triggers apoptosis in HepG2 cells.," *Avicenna J Phytomed*, vol. 8, no. 6, 2018.

[21] H. Kim and X. Xue, "Detection of total reactive oxygen species in adherent cells by 2',7'-dichlorodihydrofluorescein diacetate staining," *Journal of Visualized Experiments*, vol. 2020, no. 160, 2020.